relevant waves (planetary-scale Rossby waves) are primarily responsible for deceleration of westerlies. These waves, moreover, are far greater in vertical scale and not accurately described by the kind of slow-modulation wave theory used in models of the QBO.
17. Ten hPa is the highest pressure altitude available for all of 1958–1999.
18. N. P. Gillett, M. P. Baldwin, M. R. Allen, *J. Geophys. Res.* **105**, 7891 (2001).
19. The weak vortex events correspond closely to major stratospheric warmings, in which the normal westerly winds are replaced by easterlies at high latitudes.
20. The earliest event occurred 26 November and the latest on 23 March.
21. K. P. Shine, *Q. J. R. Meteorol. Soc.* **113**, 603 (1987).
22. The AO index was normalized by the standard deviation of daily values during December to April.
23. Monte Carlo simulations with 18 randomly selected 60-day periods beginning during December to February indicate that a mean value less than −0.44 has a probability of occurrence by chance of less than 0.003. A mean value of more than +0.35, with 30 events, also has a probability of occurrence by chance of less than 0.003.
24. We first defined the NAO spatial pattern by regressing monthly-mean 1000-hPa December to February geopotential anomalies onto Hurrell's NAO index (1958–1997). The daily NAO index is defined by projecting daily 1000-hPa geopotential anomalies onto the NAO spatial pattern. The correlation between the daily AO and NAO indices is 0.93.
25. D. W. J. Thompson, J. M. Wallace, *Science* **293**, 85 (2001).
26. From NASA's *Atlas of Extratropical Cyclones 1961–1998*.
27. Monte Carlo simulations indicate that the average latitudinal separation between the two curves (1.96°) has a probability of occurrence by chance of less than 0.001.
28. Monte Carlo simulations indicate that the average latitudinal separation between the two curves (2.94°) has a probability of occurrence by chance of less than 0.002.
29. M. P. Baldwin *et al*., *Rev. Geophys.* **39**, 179, 2001.
30. J. R. Holton, H.-C. Tan, *J. Atmos. Sci.* **37**, 2200 (1980).
31. We define the phase of the QBO by the 40-hPa equatorial wind.
32. D. W. J. Thompson, M. P. Baldwin, J. M. Wallace, in preparation.
33. W. A. Robinson, *J. Atmos. Sci.* **45**, 2319 (1988).
34. D. E. Hartley, J. T. Villarin, R. X. Black, C. A. Davis, *Nature* **391**, 471 (1998).
35. P. H. Haynes, T. G. Shepherd, *Q. J. R. Meteorol. Soc.* **115** 1181 (1989).
36. D. Ortland, T. J. Dunkerton, in preparation.
37. We thank M. A. Geller, J. R. Holton, G. N. Kiladis, M. E. McIntyre, and P. W. Mote for comments on the manuscript. Equatorial 40-hPa winds are courtesy of B. Naujokat, Freie University Berlin. Supported by the SR&T Program for Geospace Science (NASA), ACMAP Program (NASA), CLIVAR Atlantic, Office of Global Programs (NOAA), and the National Science Foundation.

11 June 2001; accepted 13 September 2001

Climatic Impact of Tropical Lowland Deforestation on Nearby Montane Cloud Forests

R. O. Lawton,[1]* U. S. Nair,[2] R. A. Pielke Sr.,[3] R. M. Welch[2]

Tropical montane cloud forests (TMCFs) depend on predictable, frequent, and prolonged immersion in cloud. Clearing upwind lowland forest alters surface energy budgets in ways that influence dry season cloud fields and thus the TMCF environment. Landsat and Geostationary Operational Environmental Satellite imagery show that deforested areas of Costa Rica's Caribbean lowlands remain relatively cloud-free when forested regions have well-developed dry season cumulus cloud fields. Further, regional atmospheric simulations show that cloud base heights are higher over pasture than over tropical forest areas under reasonable dry season conditions. These results suggest that land use in tropical lowlands has serious impacts on ecosystems in adjacent mountains.

In the Caribbean basin, as in much of the tropics, cloud forests occur where mountains force trade winds to rise above the lifting condensation level, the point of orographic cloud formation. Immersion of forest in cloud reduces solar radiation and outgoing longwave radiation, increases humidity and water inputs from mist and direct deposition of cloud droplets, and reduces transpiration (*1*, *2*). Because these actions influence soil structure, nutrient cycling, and composition of the vegetation, factors that influence the location and likelihood of cloud formation in the air masses moving over tropical mountains have profound consequences for landscape conservation and management (*1*, *3*, *4*). The Monteverde cloud forests, which are the focus of considerable conservation and research interest, provide a case in point (*2*, *5*, *6*). These lie along the crest of the Cordillera de Tilarán mountain range, which rises abruptly from the lowlands of western Costa Rica to peaks higher than 1800 m. Tropical wet forest below 700 m on the Caribbean slope grades through premontane rain forest to cloud forests at the highest elevations (*6*, *7*). The uppermost Pacific slopes are covered by lower montane wet forest, which rapidly gives way below 1500 m to a landscape that is now almost completely deforested, but was once covered with semi-evergreen premontane wet and moist forests (Fig. 1A). These transitions are largely due to the spatial pattern of dry season water inputs imposed by the orographic rise of the trade winds flowing over the Cordillera and the consequent formation of a cloud bank against the upper windward slopes (*2*, *6*, *7*). The local environmental heterogeneity produced by the geography of cloud immersion results in high levels of endemism and one of the richest floras in the world (*6*, *8*).

In the Cordillera, anuran population crashes, an increase in the upper elevation of bird ranges on the Pacific slope, and longer mist-free intervals in the dry season at the lee edge of the Monteverde cloud forest have been attributed to an increase in the base height of the orographic cloud bank (*3*). The frequency of long (≥5 days) mist-free periods in the dry season is related to Pacific sea surface temperatures, and thus to El Niño events, but a trend remains after these are considered (*3*). Based on a global climate model under $2XCO_2$ conditions, Still *et al*. (*4*) suggest that sea surface warming results in intensification of tropical hydrological cycling, with release of latent heat upon condensation, warming the atmosphere. From these results, Still *et al*. (*4*) and Pounds *et al*. (*3*) infer an increase in the lifting condensation level and the height of orographic cloud banks. Global climate models, however, have coarse spatial resolution [~400 km horizontally and several hundred meters vertically in that of Still *et al*. (*4*)] and are incapable of resolving subgrid scale features such as clouds, or terrain and land use features known to influence cloud formation.

Trade winds flow from the Caribbean, 100 km across the lowlands of the Rio San Juan basin, to the Monteverde tropical montane cloud forest (TMCF). Moving at 3 to 5 m s^{-1}, the lower atmosphere has 5 to 10 hours during which it can be influenced by the land below. Deforestation proceeded rapidly in the Costa Rican part of this basin in the past century. By 1940, a 600-km^2 area at the Caribbean foot of the Cordillera de Tilarán had been cleared (*9*). Agricultural colonization has since spread (*9*, *10*). By 1992, only about 1200 km^2 (18% of the area) of intact natural vegetation remained in the Costa Rican part of the Rio San Juan basin lowlands (*11*) (Fig. 1A). To the north of the river, the forests in southeastern Nicaragua remained largely intact.

Deforestation and conversion of land to pasture or cropland generally increase surface albedo (*12*), reduce aerodynamic roughness length and mechanically turbulent mixing in the boundary layer (*13*), reduce evapotranspiration, and increase the ratio of convective sensible

[1]Department of Biological Sciences, University of Alabama in Huntsville, Huntsville, AL 35899, USA. [2]Department of Atmospheric Science, National Space Science Technology Center, University of Alabama in Huntsville, 320 Sparkman Drive, Huntsville, AL 35806, USA. [3]Department of Atmospheric Science, Colorado State University, Fort Collins, CO 80523–1371, USA.

*To whom correspondence should be addressed. E-mail: lawtonr@email.uah.edu

heat transfers to latent heat transfers from the surface to the atmosphere (*13*). Conversion of forest to grassland or cropland also commonly alters surface soil structure by compaction (*14*) and thus reduces infiltration of rainfall and increases runoff, with the end result of reducing soil moisture. Because grasses and crops usually have shallower roots than do forest trees, the volume of water available for transpiration and latent heat transfer is greater for forests than for agricultural land developed from them (*15*, *16*). In central Amazonian rain-free dry season periods, evapotranspiration (calculated from detailed microclimatic data and energy balance calculations) from pasture declines and sensible heat transfers from pasture increase commensurately, whereas both remain constant in intact tropical forest nearby (*13*). Landscape changes that reduce evapotranspiration and increase sensible heat transfers in this manner can have climatic consequences (*17*, *18*). Overgrazing in semi-arid areas, for instance, reduces vegetation cover and produces results qualitatively similar to those outlined above (*19*). Regional atmospheric model simulations of these conditions predict reduced cloud formation and precipitation (*20*) and are corroborated by ground-based and remotely sensed observations (*19*, *20*). Conversely, irrigation of semi-arid grasslands provides reverse conditions to the original experiment by increasing the leaf area and available soil moisture, and results in increased regional cloud formation (*21*). Global climate models have suggested that tropical deforestation could decrease precipitation and increase the length of the dry season via these mechanisms (*22*, *23*).

Cumulus cloud occurrence over Nicaragua and Costa Rica during March 1999 was monitored via Geostationary Operational Environmental Satellite (GOES) visible wavelength imagery. Daily late morning (~10:15 local time) images with 1-km ground resolution were examined with a structural thresholding algorithm to detect cumulus cloud, and each pixel was classified as cumulus or not (*24*). The scenes for the month were summed by pixel to map the frequency of cumulus cloud coverage (Fig. 1C). Late morning dry season cumulus was much less abundant over the long-deforested parts of Costa Rica's Rio San Juan basin than over the nearby forested region in Nicaragua. The less thoroughly deforested areas of Costa Rica near the river showed intermediate degrees of cumulus development. Landsat images of dry season days with cumulus cloud field development in the region also showed that cumulus clouds were commonly absent or poorly developed over deforested areas (Fig. 1B). The prominent zone of reduced cumulus cloudiness in the San Carlos area lies directly upwind of the Monteverde TMCF.

To further examine the impact of regional deforestation on cumulus formation in this region, we applied the Colorado State University Regional Atmospheric Modeling System (RAMS) (*25*). In each simulation, atmospheric conditions were set initially to be horizontally homogeneous, with vertical structure dictated by data from a single radiosonde sounding (*26*). Each simulation involved a 12-hour diurnal course from roughly local dawn to dusk. Here, we present data on surface temperature, heat and moisture fluxes, and cloud base height, generated at 15-min intervals and averaged over the horizontal grid.

We used a coupled design in which each single sounding provided identical initial atmospheric structures for the forest and pasture conditions to be contrasted. We thus examined diurnally developing conditions between simulations in which the vegetation had transfer characteristics of evergreen broadleaf forest, with initial volumetric soil moisture set to 0.4, and simulations in which the vegetation had transfer characteristics of short grass (pasture) with initial volumetric soil moisture set to 0.25.

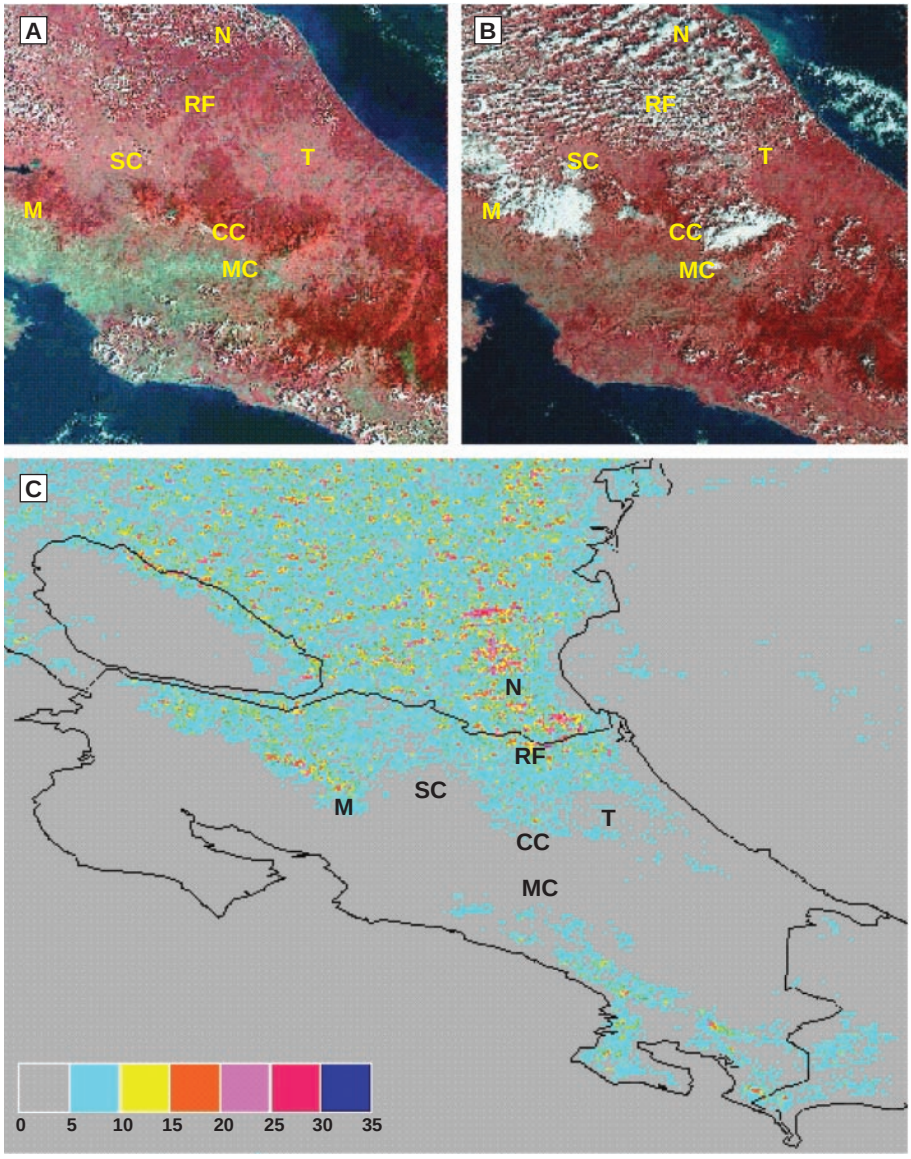

Fig. 1. Deforestation and dry season cumulus cloud cover in northern Costa Rica and southern Nicaragua. (**A**) 16:15 UTC (10:15 local time) false color Landsat image showing the long-deforested (pink) portions of the San Carlos plains (SC) and Tortuguero plains (T) upwind of the cloud forests (dark red) of Monteverde (M) and the Cordillera Volcanica Central (CC). Deforested lee (Pacific) slopes southwest of Monteverde and in the Meseta Central (MC) appear gray-green. Remnant forest (RF) remains south of the Costa Rica–Nicaragua border, whereas intact lowland forest covers southeast Nicaragua (N). (**B**)16:15 UTC false color Landsat image from a day of extensive cumulus cloud field development. Clouds have not developed over the parts of the San Carlos or Tortuguero plains that have been deforested the longest, and are less well-developed over the remnant forests of northern Costa Rica than above the adjacent forested Nicaraguan lowlands (N). (**C**) Frequency of cumulus cloud field coverage at 16:15 UTC during March 1999, compiled from daily GOES imagery, showing poor cumulus development over deforested parts of the San Carlos and Tortuguero plains.

The forest volumetric soil moisture is appropriate to tropical evergreen forest dry season surface soil in the region (*27*). Although the pasture volumetric soil moisture is lower than that observed in agricultural soil on freshly cleared land in high rainfall areas of the Caribbean lowlands (*28*), it is probably appropriate to dry season pasture in most of the area and yields results consistent with empirical micrometeorological studies of Amazonian pasture (*12*, *13*).

Our simulations suggest that conversion of forest to pasture has a significant impact on cloud formation. The differences between simulated forest and pasture surface air temperatures and sensible and latent heat transfers (Fig. 2, A through C) were similar to those observed between Amazonian forest and adjacent pasture. The greater evaporative flux over forest lowered the lifting condensation level in comparison to that over pasture and increased the convective available potential energy in air parcels. The dry season atmosphere measured by the soundings we used was such that mixing in the boundary layer became vigorous enough to initiate cloud formation in both forested and pasture scenarios by mid-morning.

Mean cloud base heights in the simulations were low early in the morning but rose throughout the day. By 10:15 local time, mean cumulus base height over forest (650 m) was substantially lower than that over pasture (1100 m) (Fig. 2D). This difference persisted until 15:30 local time. By late morning, mean cloud base height in the simulations with a pastured landscape had risen above 1800 m, higher than the peaks of the Cordillera de Tilarán. In the forested scenario, mean cloud base height did not reach 1800 m until early afternoon. These values are in reasonable agreement with observed cloud base heights in the area. In a Landsat Multispectral Scanner image from 23 March 1985 showing well-developed dry season cumulus cloud fields in the Rio San Juan basin at 10:15 local time, cloud base heights calculated trigonometrically from measurements of the displacement of matched features on the edges of clouds and their shadows (*29*) had a geometric mean of 700 m and ranged from 400 m to 1500 m.

Although these models involve cumulus generated by free convection over flat lowlands, their results are corroborated by three pairs of simulations, with realistic advection across the model boundaries, comparing completely forested and pasture scenarios over realistic terrain, provided by the U.S. Geological Survey 1-km horizontal resolution digital terrain data set (*30*). Locations of orographic clouds generated by these simulations are very similar to those observed by satellites (as in Fig. 1B). Midday orographic cloud banks in the forested case were thicker, had higher cloud: water mixing ratios, and had lower bases than in the pasture case for each pair of simulations (Fig. 3).

Reduced evapotranspiration after deforestation in tropical lowlands decreases the moisture content of the air mass flowing up the slopes of adjacent mountains. This increases the lifting condensation level and thus the elevation of the base of the cloud deck. The model results thus suggest that deforestation in the lowland tropics of the trade wind zone tends to shift the cloud forest environment upward in adjacent downwind mountains.

The scenario we present here complements that of Pounds *et al*. (*3*) and Still *et al.* (*4*),

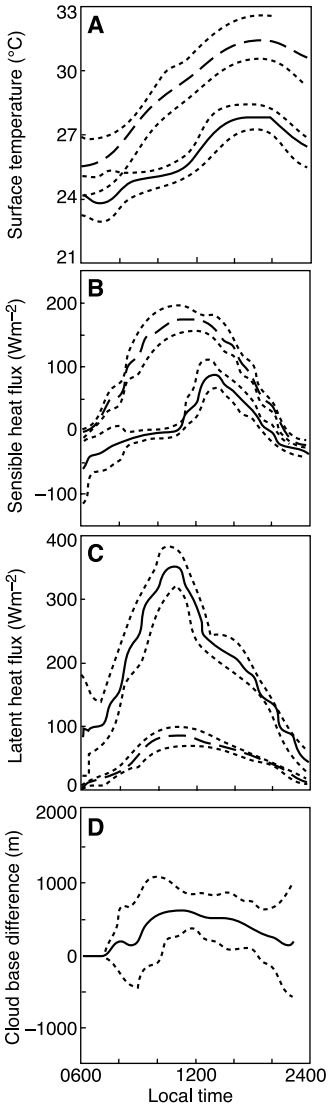

Fig. 2. Simulated dawn-to-dusk courses of (**A**) surface air temperatures, (**B**) sensible heat flux, (**C**) latent heat flux, and (**D**) difference in cumulus base heights between forested (solid lines) and pasture (dashed lines) scenarios, for Colorado State University RAMS models of forested and pasture-covered tropical lowlands. Means ± 1 SD (dotted lines) for seven model runs are presented.

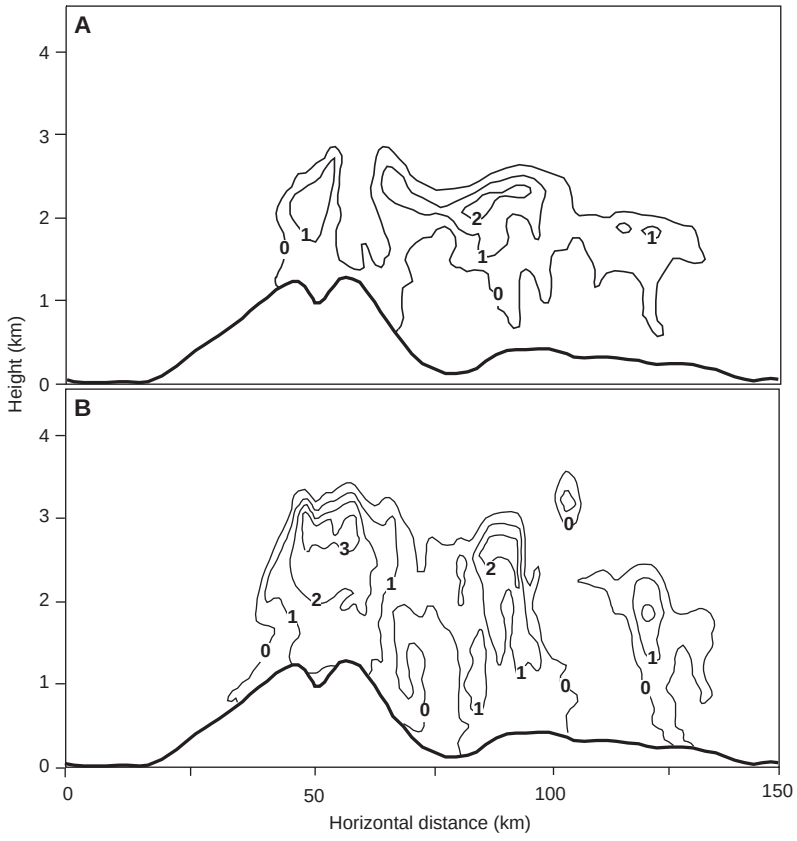

Fig. 3. West-to-east vertical cross section of the simulated cloud water mixing ratio (grams of liquid water per kilogram of air) above the Cordillera de Tilarán and adjacent lowlands at midday (11:45 local time) for initial conditions of 9 March 1999 for (**A**) a completely deforested and pastured landscape and (**B**) a completely forested landscape.

broadening the "lifting cloud base hypothesis" for biotic changes in Central American mountains, by providing an alternative mechanism—upwind deforestation of lowlands—that may increase convective and orographic cloud bases even more than changes in sea surface temperature do. Cloud forests will differ in their sensitivity to upwind deforestation and sea surface temperature changes. On the one hand, inland cloud forests like those of southern Mexico may be profoundly influenced by regional deforestation. On the other hand, coastal forests like those of some Caribbean islands (e.g., the Luquillo forest of Puerto Rico) may have too little upwind lowland to experience deforestation impacts such as those we discuss. Nonetheless, these results suggest that current trends in tropical land use will force cloud forests upward, and they will thus decrease in area and become increasingly fragmented—and in many low mountains may disappear altogether.

References and Notes

1. L. A. Bruinjzeel, J. Proctor, in *Tropical Montane Cloud Forests*, L. S. Hamilton, J. O. Juvik, F. N. Scatena, Eds. (Springer, New York, 1995), pp. 38–78.
2. K. L. Clark, R. O. Lawton, P. R. Butler, in *Monteverde: Ecology and Conservation of a Tropical Cloud Forest*, N. Nadkarni, N. Wheelwright, Eds. (Oxford Univ. Press, New York, 2000), pp. 15–38.
3. J. A. Pounds, M. P. L. Fogden, J. H. Campbell, *Nature* **398,** 611 (1999).
4. C. J. Still, P. N. Foster, S. H. Schneider, *Nature* **398,** 608 (1999).
5. N. Nadkarni, R. O. Lawton, K. L. Clark, T. J. Matelson, D. Schaefer, in *Monteverde: Ecology and Conservation of a Tropical Cloud Forest*, N. Nadkarni, N. Wheelwright, Eds. (Oxford Univ. Press, New York, 2000), pp. 303–350.
6. W. A. Haber, in *Monteverde: Ecology and Conservation of a Tropical Cloud Forest*, N. Nadkarni, N. Wheelwright, Eds. (Oxford Univ. Press, New York, 2000), pp. 39–70.
7. R. O. Lawton, V. Dryer, *Brenesia* **18,** 101 (1980).
8. N. Wheelwright, in *Monteverde: Ecology and Conservation of a Tropical Cloud Forest*, N. Nadkarni, N. Wheelwright, Eds. (Oxford Univ. Press, New York, 2000), pp. 419–432.
9. C. Vaughan, A Report on Dense Forest Habitat for Endangered Species in Costa Rica (Universidad Nacional, Heredia, Costa Rica, 1983).
10. S. A. Sader, A. T. Joyce, *Biotropica* **20**, 11 (1988).
11. E. Veldkamp, A. M. Weitz, I. G. Staritsky, E. J. Huising, *Land Degrad. Rehab.* **3**, 71 (1992).
12. H. G. Bastable, W. J. Shuttleworth, R. L. G. Dallarosa, G. Fisch, C. A. Nobre, *Int. J. Climatol.* **13**, 783 (1993).
13. I. R. Wright *et al.*, *Q. J. R. Meteorol. Soc.* **118**, 1083 (1992).
14. C. Uhl, R. Buschbacher, E. A. S. Serrao, *J. Ecol.* **76**, 663 (1988).
15. K. A. Longman, J. Jenik, *Tropical Forest and its Environment* (Longman, Harlow, UK, 1987).
16. D. C. Nepstad *et al.*, *Nature* **372**, 666 (1994).
17. Y. C. Sud, W. C. Chao, G. K. Walker, *J. Arid Environ.* **25**, 5 (1993).
18. V. M. Meher-Homji, *Clim. Change* **19**, 163 (1991).
19. W. H. Schlesinger *et al.*, *Science* **247**, 1043 (1990).
20. N. Zeng, J. D. Neelin, K.-M. Lau, C. J. Tucker, *Science* **286**, 1537 (1999).
21. F. Chen, R. Avissar, *J. Appl. Meteorol.* **33**, 1382 (1994).
22. J. Shukla, C. A. Nobre, P. Sellers, *Science* **247**, 1322 (1990).
23. C. A. Nobre, P. J. Sellers, J. Shukla, *J. Clim.* **4**, 957 (1991).
24. U. S. Nair *et al.*, *Proc. SPIE* **3750**, 345 (1999).
25. R. A. Pielke *et al.* *Meteorol. Atmos. Phys.* **49**, 69 (1992).
26. Simulations modeled atmospheric processes and surface-to-atmosphere transfers over a region 100 km by 100 km to an atmospheric elevation of 14.8 km, using a three-dimensional grid of 100 × 100 horizontal points with uniform 1-km spacing times 40 vertical points. The vertical dimension had a stretched grid, with a spacing ratio of 1.08 between successively higher intervals, so that the vertical spacing ranged from 70 m at the surface to a maximum of 750 m high in the atmosphere. Terrain in the model was flat. The lateral walls of the model space were cyclic, in the sense that transfers out through one wall entered through the opposite wall. Transfers through the top of the model space, however, were subsequently incapable of influencing modeled conditions. The soil had characteristics of a compact sandy clay loam (bulk density of 1.6 g cm^{-3}). Soil heat storage and moisture were modeled across 11 layers, and surface vegetation was modeled as a "big leaf." The radiative transfer components of the model accounted for the effects of clouds. In the simulations reported here, cloud formation processes other than those involving ice are activated but precipitation processes are not. The precipitation processes were deactivated, both to speed up the simulations and because the cloud fields simulated were mostly fair weather fields. Vertical columns with integrated liquid water contents greater than or equal to 200 g m^{-2} were considered to contain cumulus cloud. Within each such column with cumulus cloud, the cloud base height was determined as the height of the grid point with nonzero liquid water content that was closest to the surface. Because radiosonde data for the Costa Rican coastal plain were not available, we used 12:00 UTC (near local dawn) soundings from Puerto Cabezas on the northwest coast of Nicaragua, 350 km north of the Rio San Juan basin, and from San Andres island, which lies in the Caribbean 300 km northeast of Costa Rica, to initialize the atmospheric conditions for the simulations. We chose soundings for seven dry season days for which GOES imagery showed well-developed midday cumulus cloud fields in the region and minimal synoptic influences.
27. W. E. Dietrich, D. M. Windsor, T. Dunne, in *The Ecology of a Tropical Forest*, E. G. Leigh, A. S. Rand, D. M. Windsor, Eds. (Smithsonian Institution Press, Washington, DC, 1982), pp. 21–46.
28. A. M. Weitz, E. Linder, S. Frolking, P. M. Crill, M. Keller, *Soil Biol. Biochem.* **33**, 1077 (2001).
29. T. Berendes, S. K. Sengupta, R. M. Welch, B. A. Wielicki, M. Navar, *IEEE Trans. Geosci. Remote Sensing* **30,** 430 (1992).
30. These simulations used a grid 400 km by100 km centered at 10.39°N, 83.9°W in the Cordillera de Tilarán. The grid was oriented with the long axis running east to west. The horizontal grid spacing was 2 km, and the vertical varied from 30 m near the surface to 750 m higher in the atmosphere. Initial atmospheric conditions were interpolated from the National Center for Environmental Prediction (NCEP) reanalysis data (*31*) at 12:00 UTC (06:00 local time) for 3 days in March 1999. NCEP reanalysis data for 18:00 UTC and 00:00 UTC were used to adjust lateral boundary conditions during the simulation. Between 12:00 and 18:00 UTC, lateral boundary values were adjusted toward values consistent with the 18:00 UTC NCEP reanalysis data; between 18:00 and 00:00 UTC, lateral boundaries were adjusted toward the 00:00 UTC NCEP reanalysis data. Other than these differences, the model setup was similar to the previous set of simulations.
31. E. Kalnay *et al.*, *Bull. Am. Meteorol. Soc.* **77**, 437 (1996).

32. Partially supported by the NASA Earth Observing System Clouds and the Earth's Radiant Energy System (CERES) and the Advanced Spaceborne Thermal Emission and Reflection Radiometer (ASTER). We thank A. Pounds, S. Bruijnzeel, and two anonymous reviewers for discussion and comments.

11 May 2001; accepted 13 September 2001

A Fossil Lemur from the Oligocene of Pakistan

Laurent Marivaux,[1,2]* Jean-Loup Welcomme,[1] Pierre-Olivier Antoine,[3] Grégoire Métais,[1] Ibrahim M. Baloch,[2] Mouloud Benammi,[4] Yaowalak Chaimanee,[5] Stéphane Ducrocq,[1] Jean-Jacques Jaeger[1]*

In the absence of a comprehensive fossil record, the origin and early evolution of Malagasy lemurs have been subject to much uncertainty. We report here the discovery of a strepsirrhine fossil with strong cheirogaleid lemur affinities, *Bugtilemur mathesoni* gen. et sp. nov., from early Oligocene deposits of the Bugti Hills (Balochistan, Pakistan). *Bugtilemur* represents the earliest record of Lemuriformes, which hence appear to have already diversified outside of Madagascar at least 30 million years ago. This fossil clearly enhances the critical role of the Indian subcontinent in the early diversification of lemurs and constrains paleobiogeographic models of strepsirrhine lemur evolution.

The endemic Malagasy lemurs (Lemuriformes) and the Afro-Asian lorises (Lorisiformes) make up the living Strepsirrhini (*1*), the tooth-combed primates. Although these groups are widely diversified (*2*), their evolutionary history is still poorly documented. Lorisiforms have a limited fossil record extending back to the Miocene in Africa and Asia (*3*, *4*), whereas lemuriforms have so far remained unknown, with the exception of Malagasy subfossils.

Recent field expeditions in the Bugti Hills (Balochistan, Pakistan) (Fig. 1) have led to the discovery of a fossiliferous lens of fluviodeltaic sands at the Paali Nala locality in the lowermost levels of the Oligocene continental sequence (*5*). Screen washings have yielded a diverse assemblage of marine, deltaic, and aquatic invertebrates and vertebrates, together with terrestrial mammals (such as rodents, bats, insectivores, primates, carnivores, creodonts, artiodactyls, and perissodactyls). Primate fossils represent the second most diversified mammalian group after rodents. From several dozen isolated teeth, five new primate forms have been identified, in-